Solid-state NMR investigation of a heterogeneous biocatalyst using ^{1}H-detected fast magic-angle spinning at high magnetic fields

Sabu Varghese,*[a] Peter J. Halling,[b] Daniel Häussinger[c] and Stephen Wimperis*[a]

^{1}H-detected solid-state NMR experiments performed with fast magic angle spinning (75 kHz) and at high magnetic fields (B_0 = 20 T) were employed to gain structural insight into a heterogeneous biocatalyst comprising the enzyme human carbonic anhydrase II (hCA II) covalently immobilized on epoxy-silica. Two-dimensional ^{1}H-^{1}H NOESY-type correlation experiments were able to provide information on different ^{1}H environments in silica, epoxy-silica and the immobilized enzyme. Two distinct signals originating from water protons were observed; water associated with the surface of the silica and the water associated with the immobilized enzyme. Additional two-dimensional ^{1}H-^{1}H double quantum – single quantum (DQ-SQ) experiments revealed that the immobilized enzyme is not in close contact with the silica surface. Most significantly of all, comparison of two-dimensional ^{1}H-^{15}N spectra of the immobilized enzyme and the solution-state enzyme confirms that the structural integrity of the protein is well preserved upon covalent immobilization.

Introduction

Protein immobilization on solid supports and surfaces plays a crucial role in a range of technological applications including industrial biocatalysis, drug delivery, medical diagnosis, and biosensing.[1, 2] Heterogeneous biocatalysis involves the conversion of chemical or biological substances using immobilized enzymes or cells[3, 4] and is employed in industrial applications for the large scale synthesis of a wide variety of fine chemicals.[5] Little is known about the atomic-level structure of heterogeneous biocatalysts as conventional structural characterization methods, such as X-ray crystallography and solution-state NMR, cannot be directly employed. However, magic-angle spinning NMR (MAS NMR) can be used to characterize heterogeneous systems and has been demonstrated in the study of a variety of immobilized enzymes and supports.[6-15] In a similar context, it should be noted that MAS NMR has also very been successfully employed in understanding the molecular level interactions of peptides and proteins with non-biological surfaces involved in biomineralization.[16-25]

Among the various means of immobilizing enzymes on solid supports, covalent immobilization has proven to be the most stable as leaching effects of the enzyme from the support are minimized. However, the state of the enzyme and changes in its dynamics upon immobilization are not well understood. Recently, we have been able to show that the structural integrity of an enzyme was not drastically changed upon immobilization and was comparable to that in the lyophilized state by using a model enzyme human carbonic anhydrase II (hCA II) covalently immobilized on epoxy-silica.[26] Since the lyophilized state of a protein may not necessarily be identical to the native structure in solution, better insight into the native fold of the protein before and after immobilization can be obtained by comparing, for example, the two-dimensional solution-state ^{1}H-^{15}N HSQC NMR spectrum with that of the immobilized enzyme. In this research work, ^{1}H-detected solid-state NMR experiments utilizing fast magic angle spinning (75 kHz) at high magnetic fields (B_0 = 20 T) have been employed to characterize a model enzyme (hCA II) covalently immobilized on epoxy-silica. Protein samples were prepared in both isotopic natural abundance and in isotopically enriched (^{15}N) states (uniformly labelled samples termed hereafter as [U-^{15}N]/hCA II). Furthermore, to reduce spectral overcrowding in multidimensional MAS NMR experiments, hCA II samples were selectively ^{15}N labelled for the most abundant amino acid residue leucine (samples termed hereafter as [^{15}N Leu]/hCA II). Our results show that ^{1}H fast-MAS NMR can be successfully employed to characterize the different proton environments in the silica support, covalent linker and the immobilized enzyme. Comparison of two-dimensional ^{1}H-^{15}N spectrum from the immobilized enzyme and the solution-state NMR spectrum confirms that the structural integrity of the protein is well preserved upon covalent immobilization.

Experimental

Materials and sample preparation

The hCA II plasmid (pACA) used for the production of hCA II mutants was a generous gift from Carol A. Fierke (University of Michigan, USA).[27] Expression, purification, and characterization of [U-^{15}N]/hCA II and [^{15}N Leu]/hCA II were performed as described previously.[26, 28] Synthesis of epoxy-silica using SP-100-15-P Daiso silica gel and (3-glycidyloxypropyl)trimethoxysilane (GLYMO) as the covalent linker, immobilization of [U-^{15}N]/hCA II and [^{15}N Leu]/hCA II on epoxy-silica, and the biochemical characterization were performed as described previously.[26]

Solution and solid-state NMR experiments

Solution-state NMR experiments were carried out on a Bruker Avance III HD spectrometer operating at 600 MHz proton frequency, equipped with a cryogenic QCI probe $^{1}H/^{13}C/^{15}N/^{19}F$ with z-axis pulsed field gradients. Solid-state NMR experiments were performed on a Bruker Avance III 400 MHz spectrometer equipped with a widebore 9.4 T magnet and a Bruker Avance III 850 MHz spectrometer with a widebore 20 T magnet. All the experiments were performed at room temperature. The powdered dry samples were packed into 1.0 and 3.2 mm ZrO_2 rotors and were spun at frequencies of 75 and 22 kHz in 1.0 and 3.2 mm MAS probes, respectively. Chemical shifts were referenced externally relative to TMS for ^{1}H (adamantane: 1.87 ppm), ^{13}C (adamantane left peak: 38.4 ppm) and ^{15}N (glycine: 32.4 ppm). For insensitive nuclei (^{13}C and ^{15}N), pulse sequences utilized linearly ramped cross-polarization (CP)[29] and small phase incremental alternation (SPINAL)[30] ^{1}H decoupling. Two-dimensional ^{1}H-^{1}H correlation MAS NMR experiments were performed either with a NOESY-type (Nuclear Overhauser Effect SpectroscopY) sequence consisting of three simple 90° pulses or with a double-quantum – single-quantum experiment utilizing BABA (BAck-to-BAck)[31] recoupling. All the NMR data were processed using TopSpin software. Further experimental and processing details can be found in the text and figure captions.

Results and discussion

To gain a better insight into the ^{1}H environments present during different stages of enzyme immobilization, we recorded two-dimensional ^{1}H-^{1}H correlation experiments on silica, epoxy-silica and immobilized hCA II using NOESY-type pulse sequences. Fig. 1 shows two-dimensional ^{1}H-^{1}H NOESY spectra of (a) silica, (b) epoxy-silica, (c) [U-^{15}N]/hCA II immobilized on epoxy-silica and (d) [^{15}N Leu]/hCA II immobilized on epoxy-silica recorded using a mixing time of 100 ms on a B_0 = 20 T magnet at a MAS frequency of 75 kHz. The spectra are well resolved and reveal diagonal peaks and off-diagonal or cross peaks; the latter may arise from either chemical exchange or from spin diffusion (indicating nuclei close in space, 0.2-0.5 nm) during the mixing time.

The NOESY spectrum of bare silica (Fig. 1a) features diagonal peaks appearing from isolated silanol groups (iOH, 1.1, 2.1 ppm), adsorbed water (H_2O, 4.0 ppm) and hydrogen-bonded silanol groups (hBS, 4.5 to 9.0 ppm). The chemical shift assignments are based on the labelling scheme shown in Fig. 2, where the simplified representation of the hydrogen bonding of water with surface silanol groups is based on previous reports.[32] The peak from adsorbed water (4.0 ppm) is relatively narrow when compared with the broad peak from the hBS (4.5 to 9. 0 ppm) indicating the presence of dynamics to average out anisotropic interactions. The peak broadening from the hBS (4.5 to 9.0 ppm) can be ascribed to the absence of dynamics and the inhomogeneous broadening associated with a wide range of chemical shifts contributed by the different modes of hydrogen bonding between surface silanol groups.[33] Strong cross peaks can be observed (4.0 ppm – 4.5 to 9.0 ppm) between adsorbed water and hBS, indicating that hydrogen-bonded silanol groups are associated with strong dipolar interactions with adsorbed water revealing their proximities in space. The spectrum also reveals cross peaks between iOH and adsorbed water (1.1 – 4.0 ppm) and, with low intensity, between hBS and iOH (7.6 – 1.1 ppm), shown by dotted grey boxes. The weak cross peak probably arises from spin diffusion due to the relatively long mixing time (100 ms) used.

The two-dimensional spectrum of epoxy-silica (Fig. 1b) is well resolved and shows diagonal peaks from the epoxy-linker (0 – 3.5 ppm), adsorbed water (4.0 ppm) and hBS groups (4.5 – 10.0 ppm). The spectrum also reveals cross peaks between protons from the epoxy-linker, as shown by the green labels. Strong cross peaks can also be observed between hBS and various protons (1, 2, 3, 4, 5, $SiOCH_3$) from the epoxy-linker. This could be a result of the relatively long mixing time (100 ms) used, as spin diffusion can result in long-range magnetization transfer and can generate cross-peaks between all linker protons. It is worth noting the weak cross peak (below the contour levels on one side of the diagonal) between the H_6 from the epoxy-ring (2.4 ppm) and the hBS groups (5.5 ppm), highlighted in yellow. This indicates that some of the epoxy groups have opened to form diols and are in close proximity with hBS groups on the surface of silica. [This was further confirmed by comparison of two-dimensional ^{1}H-^{13}C HETCOR spectra of the epoxy-silica recorded at short (0.4 ms, red contour levels) and long (4 ms, black contour levels) CP contact times (Fig. 3), with the latter spectrum showing a very weak cross peak (highlighted with the green circle) between protons from the water (4.0 ppm) and carbons from the opened epoxy groups (6_{op}).] Finally, partly resolved cross peaks (0.8 – 4.0 ppm), (1.4 – 4.0 ppm), (3.0 – 4.0 ppm) can be observed in Fig. 1b between the protons from the H1, H2 and H3/H4/H5/$SiOCH_3$ groups in the epoxy-linker with the adsorbed water (highlighted in red). In this context it is worth noting the downfield shift of the H1 protons of the epoxy linker from 0.4 to 0.8 ppm indicating the possibility of weaker interactions with the adsorbed water. However, no noticeable changes in chemical shifts could be observed for the H2 and H3/H4/H5/$SiOCH_3$ groups from the epoxy-linker. Further cross peaks can be observed (1.0 – 1.8 ppm) between H1 and H2 with the adsorbed water (4.0 ppm). Note that, although synthesis of epoxy-silica was performed under non-aqueous conditions, the peak at 4.0 ppm can be ascribed to adsorbed water from the atmosphere due to the hygroscopic nature of silica.

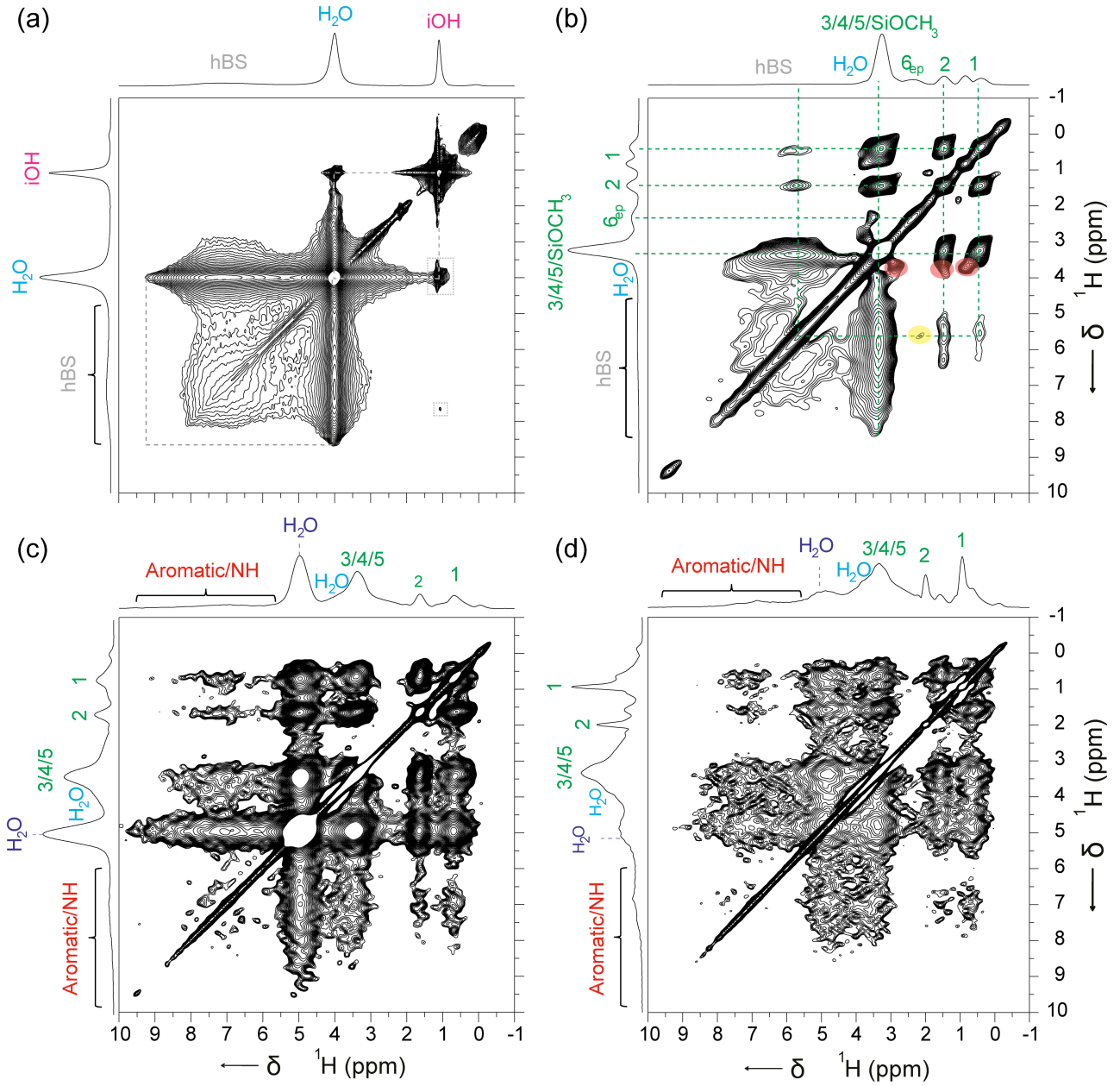

Fig. 1. Two-dimensional (^{1}H-^{1}H) correlation NOESY-type spectra of (a) silica, (b) epoxy-silica, (c) [U-^{15}N]/hCA II immobilized on epoxy-silica and (d) [^{15}N Leu]/hCA II immobilized on epoxy-silica. The spectra were recorded using 100 ms mixing time on a B_0 = 20 T magnet at a MAS frequency of 75 kHz. All spectra were acquired using 8 transients for each of 300 t_1 increments of 53.3 µs using a recycle interval of 2 s. Spectrum (a) was processed with 50 Hz line broadening in both F1 and F2 dimensions; the remainder were processed using line broadening of –150 Hz and Gaussian broadening of 0.2 in both F1 and F2 dimensions. The chemical shift assignments are based on the numbering scheme shown in Fig. 2. The cross peaks highlighted in red and yellow are discussed in the text.

The ^{1}H NOESY spectra of [U-^{15}N]/hCA II (Fig. 1c) and [^{15}N Leu]/hCA II (Fig. 1d) immobilized on epoxy-silica are almost identical and reveal diagonal peaks from the epoxy-linker (0 – 3.5 ppm), water (4.0, 5.0 ppm) and from the aromatic and amide protons in the immobilized enzyme (6 – 10 ppm), highlighted with green, blue and red labels respectively. It is worth noting the two distinct water peaks at 4 and 5 ppm. The partly resolved water peak at 4 ppm can be ascribed to water associated with the surface of the epoxy-silica, while the water peak at 5 ppm can be ascribed to water associated with the immobilized enzyme (protein-associated water is usually observed at ~4.7 ppm).[34] These spectra also reveal cross peaks between protons from the epoxy-linker (0 – 4 ppm), epoxy-linker and water (0 to 4 ppm – 5 ppm), epoxy-linker and hCA II (0 to 4 ppm – 6 to 10 ppm), and also between water and hCA II (5 – 6 to 10 ppm).

For gaining further insight into the more strongly dipolar coupled protons, two-dimensional ^{1}H double-

quantum – single quantum (DQ-SQ) experiments using BABA recoupling were recorded. The DQ MAS NMR experiments selectively excite ^{1}H nuclei that are strongly dipolar coupled and, as a result, mobile or isolated protons are normally not observed. Fig. 4 shows the ^{1}H DQ MAS NMR spectra of (a) epoxy-silica, (b) [U-^{15}N]/hCA II immobilized on epoxy-silica and (c) [^{15}N Leu]/hCA II immobilized on epoxy-silica recorded at room temperature with one rotor period of recoupling on a B_0 = 20 T magnet at a MAS frequency of 75 kHz. Our DQ experiments on silica were unsuccessful as the recoupling was inefficient due to the mobility of the water molecules (data not shown).

Fig. 2. Simplified schematic representation of (a) bare silica, (b) epoxy-silica before immobilization and (c) epoxy-silica after immobilization with hCA II. Two possible modes of connection of the linker to the silica surface are shown in (b) and (c).

The DQ spectrum of epoxy-silica (Fig. 4a) is well resolved and reveals pairs of correlated peaks, with the same F1 frequency and equidistant from the +2 diagonal, arising from protons that are close in space. The DQ-SQ

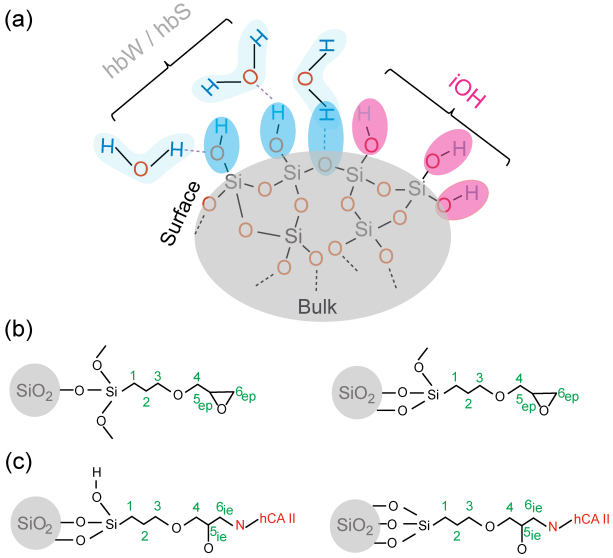

correlation peaks between protons from the epoxy-linker are shown connected by dotted green lines, while the correlation peaks between protons in the epoxy-linker and the hBS groups are shown connected by dotted cyan lines. Well-resolved pairs of correlation peaks are observed between H1 – H2 (0.4 –1.4 ppm), H1-SiOCH$_3$ (0.4 – 3.1 ppm) and H2-H3 (1.4 – 3.3 ppm) groups revealing their close proximities in space. The unsymmetrical peaks appearing around 3.5 ppm in F2 probably arise as a result of t_1 noise from the adsorbed water.

The DQ spectra of [U-^{15}N]/hCA II immobilized on epoxy-silica (Fig. 4b) and [^{15}N Leu]/hCA II immobilized on epoxy-silica (Fig. 4c) are almost identical and consists of pairs of correlation peaks from the epoxy-linker, H1 – H2 (0.4 – 1.4 ppm), H2 – H3 (1.4 – 3.3 ppm), plus a range of correlation peaks connecting H3, H4, H5 and the immobilized hCA II (shown with dotted red lines). Interestingly, we do not observe any correlation peaks connecting H1 and H2 protons in the epoxy-linker with protons from the immobilized hCA II, indicating that these protons are not close in space. Normally, H1 and H2 protons in the epoxy linker are found close to the silica surface and the absence of any correlation peaks may indicate that immobilized enzyme is not in close contact with silica surface. Thus the epoxy-linker might be acting as a cushion between the silica surface and the protein, thereby preventing any strong charge interactions that might lead to protein denaturation. Similar studies involving reconstitution of transmembrane proteins anchored into polymer-supported cushioned lipid bilayers have shown increased incorporation and enhanced enzymatic activity when compared to the reconstituted enzyme.[35]

Fig. 3. Overlay of the two-dimensional ^{1}H-^{13}C HETCOR spectra of epoxy-silica recorded on a B_0 = 9.4 T spectrometer at a MAS frequency of 22 kHz using a ^{1}H-^{13}C CP contact time of 0.4 ms (red contours) and 4 ms (black contours). Each spectrum was acquired using 1024 transients for each of the 128 t_1 increments of 250 µs. High-power homo- and heteronuclear proton decoupling (~90 kHz) was applied during the FSLG (Frequency-Switched Lee–Goldberg)[36-39] τ intervals during ^{13}C acquisition. Both spectra were processed without any window functions.

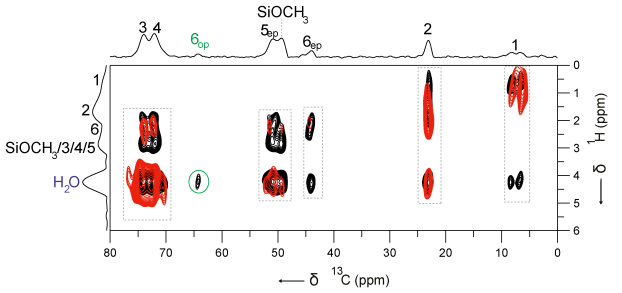

Projections are shown only from the spectrum with longer mixing time (4 ms). Chemical shift assignments are based on previous reports.[9, 26] The cross peak corresponding to opened epoxy groups (6_{op}) is highlighted in green.

Fig. 4. Two-dimensional (^{1}H-^{1}H) DQ-SQ spectra of (a) epoxy-silica, (b) [U-^{15}N]/hCA II immobilized on epoxy-silica and (c) [^{15}N Leu]/hCA II immobilized on epoxy-silica recorded on a B_0 = 20 T magnet at a MAS rate of 75 kHz. All spectra were acquired using 16 transients for each of the 128 t_1 increments of 13.3 µs using a recycle interval of 2 s. The spectra were processed using line broadening of –150 Hz and Gaussian broadening of 0.2 in both F1 and F2 dimensions. The chemical shift assignments are based on the numbering scheme shown in Fig. 2.

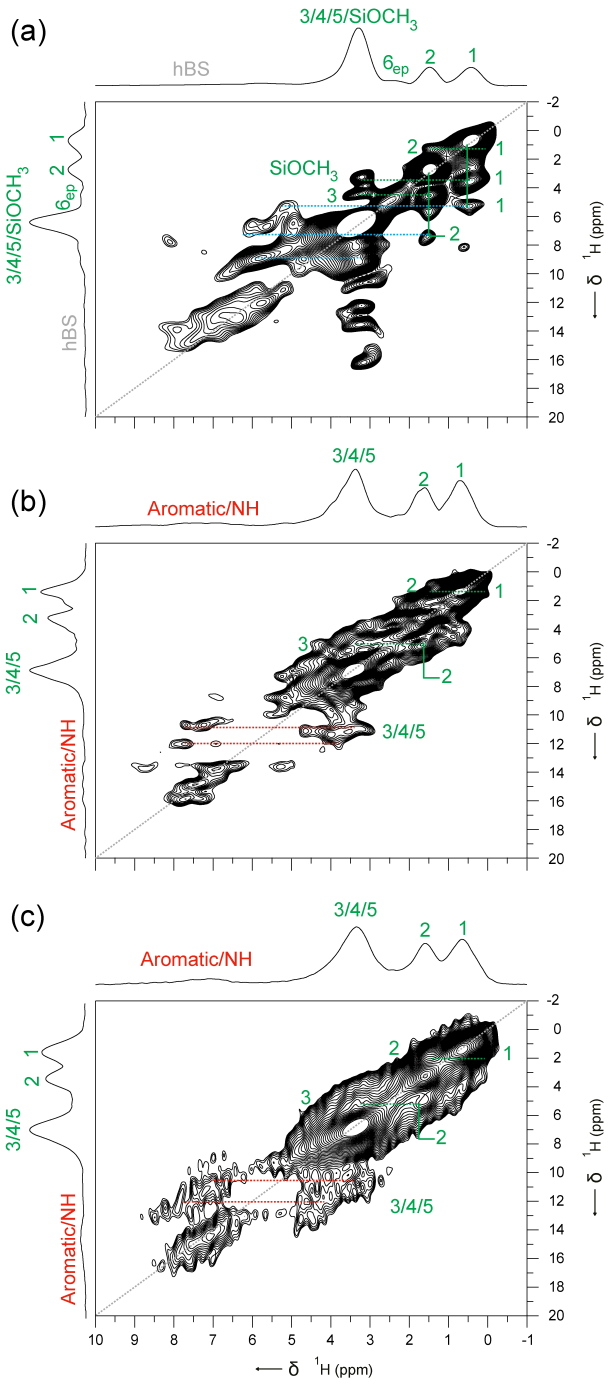

In order to help understand the state of the enzyme after immobilization, a ^{1}H-detected fast MAS NMR (^{1}H-^{15}N) correlation experiment was recorded. Fig. 5 compares the resulting spectrum of [U-^{15}N]/hCA II in the immobilized state (Fig. 5b) with the solution-state TROSY-HSQC (Transverse Relaxation-Optimized Spectroscopy - Heteronuclear Single Quantum Coherence)[40] NMR spectrum of hCA II (Fig. 5a). Comparison of the two spectra reveals that majority of the peaks in the central region are well preserved and the overall distribution of the peaks from the immobilized hCA II indicates that the structural integrity of the enzyme is well preserved on immobilization. Additional high frequency peaks (> 11 ppm in the ^{1}H dimension) in the immobilized state can be ascribed to strong hydrogen bonds in the solid that are broken upon dissolution.

Fig. 5. (a) Solution-state TROSY[40]-HSQC NMR spectrum of hCA II and (b) ^{1}H-detected (^{1}H-^{15}N) MAS NMR spectrum of [U-^{15}N]/hCA II in the immobilized state. The solution-state NMR spectrum of the [U-^{15}N]/hCA II was acquired using 64 transients for each of the 256 t_1 increments of 500 µs using a recycle interval of 1 s on a B_0 = 14.1 T magnet. The spectrum of the [U-^{15}N]/hCA II in the immobilized state was acquired using 1024 transients for each of the 40 t_1 increments of 290 µs using a recycle interval of 2 s on a B_0 = 20 T magnet at a MAS frequency of 75 kHz. The spectra

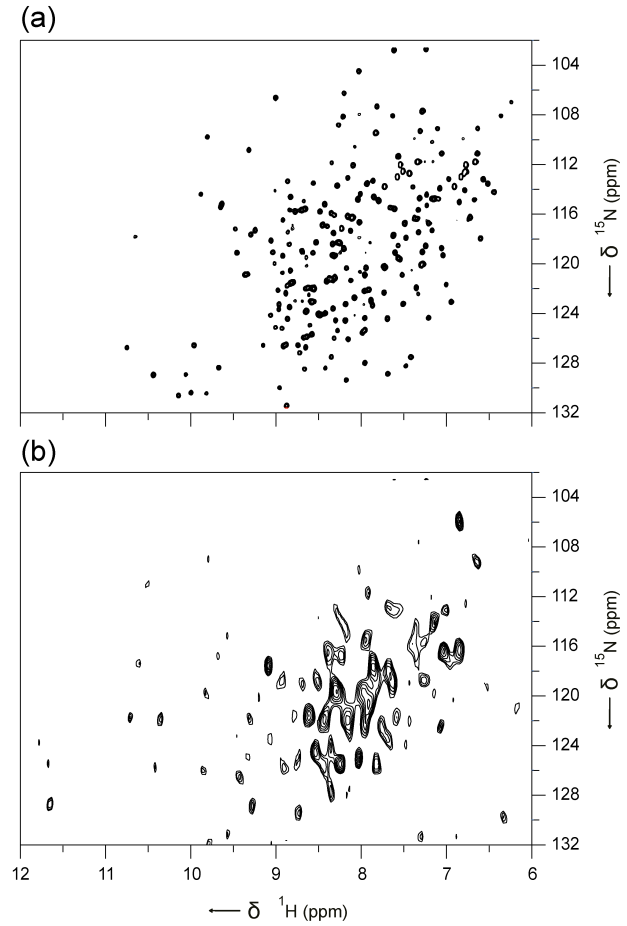

were processed without any window functions.

Overall, a smaller number of resonances are observed from the hCA II in the immobilized state compared with the solution-state NMR HSQC spectrum. The solution-state HSQC NMR experiment is based on INEPT-type (Insensitive Nuclei Enhanced by Polarization Transfer) coherence transfer through J couplings, which works efficiently for many liquid samples. In NMR of solids, INEPT signals from proteins are normally observed from residues that have sufficient mobility to average out anisotropic interactions and yield narrow resonances. We did not observe any signals from immobilized hCA II using INEPT-based experiments (data not shown). In contrast, ^{1}H-detected

MAS NMR experiments rely on cross polarization (CP) via heteronuclear through-space dipolar couplings,[29] which works efficiently for rigid solid samples. It seems likely that the absence of many cross-peak signals in Fig. 5b can be attributed to static disorder leading to enhanced line broadening, as has been reported previously in the case of proteins entrapped in bioinspired silica.[18] It should be noted that, although we are suggesting that the structural integrity of the enzyme is well preserved on immobilization, this does not mean that the sample is not highly disordered. Individual proteins molecules can be expected to be tethered to the silica surface by a variable number of linker molecules and to have a very wide range of orientations with respect to the surface, which itself will be highly heterogeneous. ^{1}H-detected experiments on [^{15}N Leu]/hCA II immobilized on epoxy-silica were not successful (data not shown) due to the fewer expected resonances (26 Leu residues) consequent upon selective ^{15}N isotopic labelling and to the limited experimental sensitivity arising from the smaller amount of protein grafted on to the surface of the epoxy-silica support (9.9 mg of protein per 100 mg of support).[26]

Conclusions

In conclusion, we have demonstrated that ^{1}H-detected solid-state NMR experiments at high magnetic fields and utilizing fast MAS can be successfully employed to gain insight into the ^{1}H environments from silica, epoxy-silica and enzymes covalently immobilized on epoxy-silica. Most importantly, our results show that structural integrity of the protein is not drastically changed, but is well preserved upon covalent immobilization. This relates to our previous observation that this immobilized enzymatic system retains 71% of its effective specific activity when compared with free hCA II in solution.[26] The outcomes of this present work are therefore not limited to the better understanding of heterogeneous biocatalysts, but also to wider areas of biotechnological processes and applications involving interactions of proteins with solid surfaces and supports.

Conflicts of interest

There are no conflicts to declare.

Acknowledgements

We thank the Leverhulme Trust (award RPG-2013-361) for financial support. We are indebted to Dr Kaspar Zimmermann for preparation of all protein constructs, Dr Elisa Nogueira for assistance, and the Swiss National Science Foundation for a grant to DH (SNF 200021_130263). The UK 850 MHz Solid-State NMR Facility used in this research was funded by EPSRC and BBSRC (contract reference PR140003), as well as the University of Warwick including via partial funding through Birmingham Science City Advanced Materials Projects 1 and 2 supported by Advantage West Midlands (AWM) and the European Regional Development Fund (ERDF). Collaborative assistance from the 850 MHz Facility Manager (Dr. Dinu Iuga, University of Warwick) is gratefully acknowledged. We also thank Daiso Chemical Co. Ltd, Japan, for donating the silica support used in this research.

Notes and references

1. A. Kuchler, M. Yoshimoto, S. Luginbuhl, F. Mavelli and P. Walde, *Nat. Nanotechnol.*, 2016, **11**, 409-420.
2. F. Rusmini, Z. Zhong and J. Feijen, *Biomacromolecules*, 2007, **8**, 1775-1789.
3. D. N. Tran and K. J. Balkus, *ACS Catal.*, 2011, **1**, 956-968.
4. R. A. Sheldon and S. van Pelt, *Chem. Soc. Rev.*, 2013, **42**, 6223-6235.
5. R. DiCosimo, J. McAuliffe, A. J. Poulose and G. Bohlmann, *Chem. Soc. Rev.*, 2013, **42**, 6437-6474.
6. P. Xue, F. Xu and L. Xu, *Appl. Surf. Sci.*, 2008, **255**, 1625-1630.
7. M. Park, S. S. Park, M. Selvaraj, D. Zhao and C.-S. Ha, *Microporous Mesoporous Mater.*, 2009, **124**, 76-83.
8. S. B. Hartono, S. Z. Qiao, J. Liu, K. Jack, B. P. Ladewig, Z. Hao and G. Q. M. Lu, *J. Phys. Chem. C*, 2010, **114**, 8353-8362.
9. N. E. Fauré, P. J. Halling and S. Wimperis, *J. Phys. Chem. C*, 2014, **118**, 1042-1048.
10. J. M. Bolivar, I. Eisl and B. Nidetzky, *Catal. Today*, 2016, **259**, Part 1, 66-80.
11. L. Cerofolini, S. Giuntini, A. Louka, E. Ravera, M. Fragai and C. Luchinat, *J. Phys. Chem. B*, 2017, **121**, 8094-8101.
12. T. Weidner, N. F. Breen, K. Li, G. P. Drobny and D. G. Castner, *Proc. Natl. Acad. Sci. U.S.A.*, 2010, **107**, 13288-13293.
13. Z. Zhou, F. Piepenbreier, V. R. R. Marthala, K. Karbacher and M. Hartmann, *Catal. Today*, 2015, **243**, 173-183.
14. C. Guo and G. P. Holland, *J. Phys. Chem. C*, 2015, **119**, 25663-25672.
15. P. V. Bower, E. A. Louie, J. R. Long, P. S. Stayton and G. P. Drobny, *Langmuir*, 2005, **21**, 3002-3007.
16. W. J. Shaw, *Solid State Nucl. Magn. Reson.*, 2015, **70**, 1-14.
17. T. Martelli, E. Ravera, A. Louka, L. Cerofolini, M. Hafner, M. Fragai, C. F. W. Becker and C. Luchinat, *Chem. Eur. J.*, 2016, **22**, 425-432.
18. E. Ravera, L. Cerofolini, T. Martelli, A. Louka, M. Fragai and C. Luchinat, *Sci. Rep.*, 2016, **6**, 27851.
19. E. Ravera, T. Martelli, Y. Geiger, M. Fragai, G. Goobes and C. Luchinat, *Coord. Chem. Rev.*, 2016, **327**, 110-122.
20. E. Ravera, V. K. Michaelis, T.-C. Ong, E. G. Keeler, T. Martelli, M. Fragai, R. G. Griffin and C. Luchinat, *ChemPhysChem*, 2015, **16**, 2751-2754.
21. G. Goobes, P. S. Stayton and G. P. Drobny, *Prog. Nucl. Magn. Reson. Spectrosc.*, 2007, **50**, 71-85.
22. M. J. Duer, *J. Magn. Reson.*, 2015, **253**, 98-110.
23. W. Y. Chow, R. Rajan, K. H. Muller, D. G. Reid, J. N. Skepper, W. C. Wong, R. A. Brooks, M. Green, D. Bihan, R. W. Farndale, D. A. Slatter, C. M. Shanahan and M. J. Duer, *Science*, 2014, **344**, 742-746.
24. S. I. Brückner, S. Donets, A. Dianat, M. Bobeth, R. Gutiérrez, G. Cuniberti and E. Brunner, *Langmuir*, 2016, **32**, 11698-11705.
25. X. Yang, F. Huang, X. Xu, Y. Liu, C. Ding, K. Wang, A. Guo, W. Li and J. Li, *Chem. Mater.*, 2017, **29**, 5663-5670.

26. S. Varghese, P. J. Halling, D. Häussinger and S. Wimperis, *J. Phys. Chem. C*, 2016, **120**, 28717-28726.
27. S. K. Nair, T. L. Calderone, D. W. Christianson and C. A. Fierke, *J. Biol. Chem.*, 1991, **266**, 17320-17325.
28. L. Zheng, U. Baumann and J.-L. Reymond, *Nucleic Acids Res.*, 2004, **32**, e115.
29. A. Pines, M. G. Gibby and J. S. Waugh, *J. Chem. Phys.*, 1973, **59**, 569-590.
30. B. M. Fung, A. K. Khitrin and K. Ermolaev, *J. Magn. Reson.*, 2000, **142**, 97-101.
31. W. Sommer, J. Gottwald, D. E. Demco and H. W. Spiess, *J. Magn. Reson., Ser. A*, 1995, **113**, 131-134.
32. B. Grünberg, T. Emmler, E. Gedat, I. Shenderovich, G. H. Findenegg, H.-H. Limbach and G. Buntkowsky, *Chem. Eur. J*, 2004, **10**, 5689-5696.
33. G. E. Maciel, *J. Am. Chem. Soc.*, 1996, **118**, 401-406.
34. A. Lesage and A. Böckmann, *J. Am. Chem. Soc.*, 2003, **125**, 13336-13337.
35. L. Renner, T. Pompe, R. Lemaitre, D. Drechsel and C. Werner, *Soft Matter*, 2010, **6**, 5382-5389.
36. M. Lee and W. I. Goldburg, *Phys. Rev.*, 1965, **140**, A1261-A1271.
37. B. J. van Rossum, H. Förster and H. J. M. de Groot, *J. Magn. Reson.*, 1997, **124**, 516-519.
38. A. Ramamoorthy, C. H. Wu and S. J. Opella, *J. Magn. Reson. B*, 1995, **107**, 88-90.
39. A. Ramamoorthy, C. H. Wu and S. J. Opella, *J. Magn. Reson.*, 1999, **140**, 131-140.
40. K. Pervushin, R. Riek, G. Wider and K. Wüthrich, *Proc. Natl. Acad. Sci. U.S.A.*, 1997, **94**, 12366-12371.